

Effect of severe plastic deformation on creep behaviour and microstructure changes of P92 at 923 K

P. Král^{1*}, J. Dvořák¹, V. Sklenička¹, T. Masuda², Y. Tang³, Z. Horita^{3,4,5}, L. Kunčická¹,
K. Kuchařová¹, M. Kvapilová¹, M. Svobodová⁶

¹*Institute of Physics of Materials, Academy of Sciences of the Czech Republic, Žitkova 22, 616 62 Brno, Czech Republic*

²*Department of Mechanical Engineering and Materials Science, Yokohama National University, Yokohama 240-8501, Japan*

³*Kyushu Institute of Technology, Kitakyushu 804-8550, Japan*

⁴*Magnesium Research Center, Kumamoto University, Kumamoto 860-8555, Japan*

⁵*Saga University, Synchrotron Light Application Center, Saga 840-8502, Japan*

⁶*UJP PRAHA a.s., 156 10 Prague-Zbraslav, Czech Republic*

Received 27 April 2021, received in revised form 6 May 2021, accepted 21 May 2021

Abstract

The creep behaviour of P92 steel at 923 K, deformed by rotary swaging (RS) and high-pressure torsion (HPT), was investigated. The RS-processed state contained extremely inhomogeneous microstructure containing large elongated and fine, more or less equiaxed grains. By contrast, the HPT-processed state consists of homogeneous fine-grained microstructure. It was found that both the microstructures coarsen not only with the increasing creep time but also with creep strain. The creep strain significantly accelerates the coarsening of the microstructure, especially in the HPT-processed state. The grain coarsening during creep leads to the change of the creep rate stress exponent n thus to the change of creep mechanism. The value of n depends on the ratio grain versus stationary subgrain size. P92 steel processed by RS and HPT exhibited faster $\dot{\epsilon}_{\min}$ and higher ductility compared to coarse-grained (CG) state. However, RS-processed P92 steel can exhibit at high stresses similar creep behaviour as CG state.

Key words: creep-resistant 9% Cr steels, severe plastic deformation, creep, microstructure

1. Introduction

Martensitic heat resistant 9% Cr steels are important structural materials for components of power plants working at temperatures about 873 K [1, 2]. A new generation of ultra-supercritical power plants can be operated even at temperatures about 923 K. Creep behaviour of 9% Cr steels is significantly deteriorated by coarsening of subgrains and carbides, recovery of martensite, and by the formation of secondary phases such as Laves phase and Z phase [1–5].

After normalization and tempering martensitic 9% Cr steels have a fine subgrain microstructure with high dislocation density in the interiors which slows creep rate down [1, 5]. The subgrains size coarsen with creep strain until their size reaches a station-

ary value expected for the stationary state [5–7]. The stationary state is the state when stress and strain rate is constant. However, during creep testing under the constant load, the stress and also creep strain are changing. For this reason, the so-called stationary state is sometimes called quasi-stationary (qs) because the changing stress and creep strain lead to small but not negligible microstructure changes [7–9].

Under certain creep loading conditions (high temperature and/or low stresses), the estimated stationary subgrain size can be comparable or even larger than the spacing of high-angle boundaries [10–12]. This situation can occur in fine-grained microstructures, which can be found in real components such as fine-grained regions in the heat-affected zones of the welds [13] or surfaces of tubes processed by shot

*Corresponding author: e-mail address: pkral@ipm.cz

peening [14]. Relevant creep processes can be investigated in materials processed by severe plastic deformation (SPD) [11]. The methods of SPD produce materials with the various number of low-angle (LA) and high-angle (HA) grain boundaries (GBs). The number of LAGBs and HAGBs depends on the imposed value of the shear strain [15]. The microstructures after low values of imposed plastic strain usually contain cells and subgrains with LAGBs. However, in the case that extremely large deformation is imposed on the material, the transformation of CG microstructure to ultrafine-grained (UFG) one (grain size 0.1–1 μm) occurs [16]. Thus SPD method provides a unique opportunity to study creep in the microstructures containing either subgrain or grain microstructure predominantly. The aim of the present work is an experimental study of microstructure and creep behaviour of P92 steel processed by SPD and tested at 923 K. The experimental results are compared with the creep behaviour of standard (coarse-grained) P92 steel.

2. Experimental material and procedures

The experimental material used in the present work was advanced tungsten modified 9%Cr P92 steel. The chemical composition and heat treatment of the as-received coarse-grained state are given elsewhere [17]. Discs of 30 mm diameter and 1.1 mm thickness were cut from as-received P92 steel. The discs were processed by 1 rotation high-pressure torsion (HPT) at room temperature under the pressure of 6 GPa and rotation speed of 0.1 rpm. The value of von Mises equivalent strain during HPT [15] increases with the distance r from the disc centre according to $\varepsilon_{\text{eq}} = 2\pi r N / \sqrt{3}t$, where N is the number of turns and t is the thickness of the disc. The equivalent strain imposed (deformation degrees) by rotary swaging (RS) [18, 19] was estimated by $\varepsilon_{\text{eq}} = \ln(D_0/D_n)^2$, where D_0 is the initial diameter ~ 30 mm and D_n is the final diameter ~ 15 mm after application of RS at room temperature.

Constant load tensile creep tests were conducted at 923 K in a protective argon atmosphere using flat specimens with a gauge length of 10 mm and a cross-section of $3 \times 1 \text{ mm}^2$. The tested HPT-processed specimen for the creep testing were manufactured from the disc region with an equivalent strain of about 20–30 [20, 21]. Microstructure investigations were performed using a scanning electron microscope (SEM, Tescan Lyra 3 equipped with NordlysNano EBSD detector operating at accelerating voltage of 20 kV with specimen tilted at 70°). EBSD was used to determine the misorientations θ between neighbouring grains. $\theta = 15^\circ$ was taken to distinguish HAGBs from LAGBs. The mean spacing of LAGBs along test lines is called w , the mean spacing of HAGBs is called d .

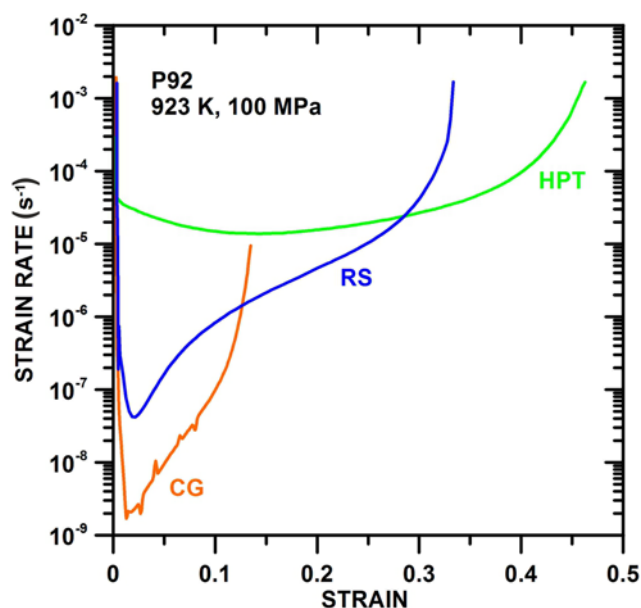


Fig. 1. Comparison of creep behaviour of CG, RS and HPT-processed states tested at 100 MPa.

3. Experimental results

3.1. Creep behaviour

Figure 1 shows the strain rate vs strain curves for coarse-grained P92 and SPD-processed states tested at 923 K and initial stress of 100 MPa. One can see that the strain to fracture is higher in the states processed by HPT and RS in comparison with the CG state.

Comparing the creep curves indicates that the RS-processed P92 steel exhibits a pronounced softening after reaching the minimum strain rate $\dot{\varepsilon}_{\text{min}}$ (Fig. 1). The softening after the reaching $\dot{\varepsilon}_{\text{min}}$ slows down with a further increase of the creep strain before creep fracture processes occur.

Figure 2 shows the creep curves of strain rate vs strain measured at different applied stresses. One can see that strain to fracture increases with decreasing applied stress in the investigated stress range. The creep curves for tests carried out at medium stresses (with $\dot{\varepsilon}_{\text{min}}$ in the range of 10^{-7} – 10^{-8} s^{-1}) exhibit a pronounced $\dot{\varepsilon}_{\text{min}}$. The results demonstrate that the pronounced $\dot{\varepsilon}_{\text{min}}$ is shifted, with decreasing applied stress, to the smaller creep strains. It means that creep strain during the primary (transient) creep stage shortens with decreasing stress. The softening after reaching of $\dot{\varepsilon}_{\text{min}}$ becomes less pronounced with decreasing stress level.

Thus up to 3 different regions can be found in the tertiary creep stage. The steep increase of strain rate after $\dot{\varepsilon}_{\text{min}}$ is often linked to the fracture processes. However, if the deformation is fairly uniform after

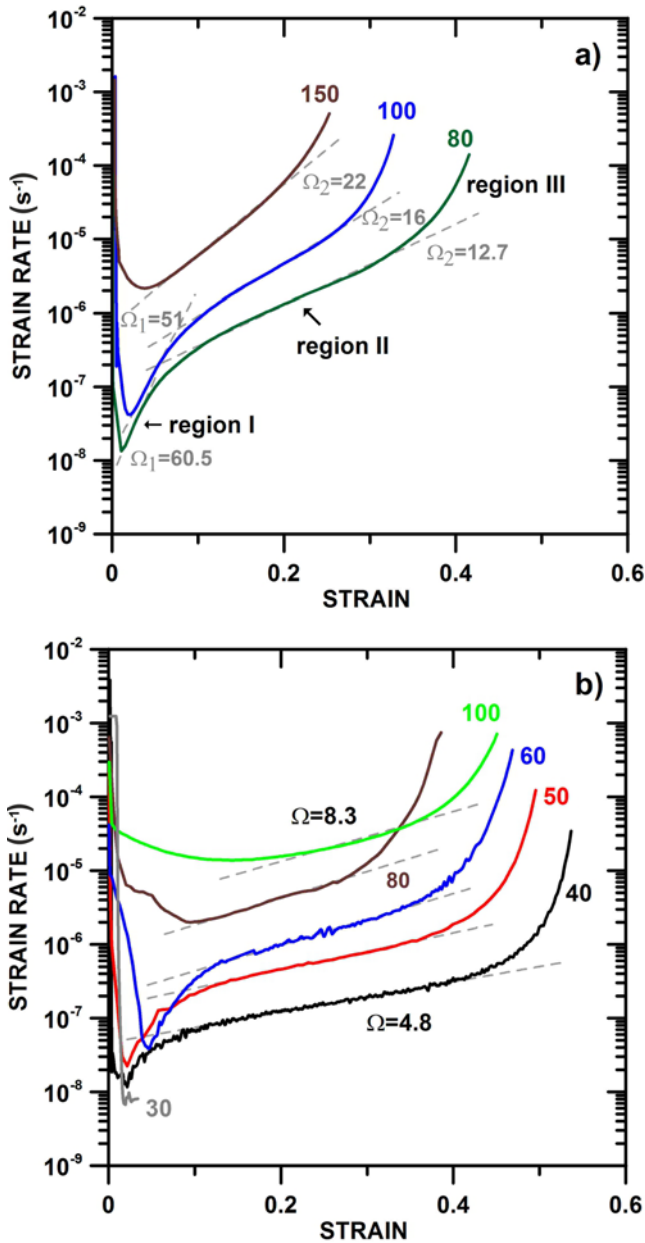


Fig. 2. Creep curves strain rate vs. strain for: a) RS and b) HPT-processed states.

$\dot{\epsilon}_{\min}$, the rate increase should be attributed to softening by internal microstructural changes.

The slope change can be indicated by the deviation of the experimental creep curves from dashed grey lines in Fig. 2. The dashed lines indicating the slope of the creep curves may be characterized by coefficient $\Omega = d \ln \dot{\epsilon} / d \epsilon$ [22], where d is the other parameter associated with damage, such as creep voids. The coefficient Ω may also be referred to as n' [8]. Region I is characterized by a pronounced softening, and the coefficient Ω achieved quite high values about 40–60 for SPD-processed states. Region I was not observed

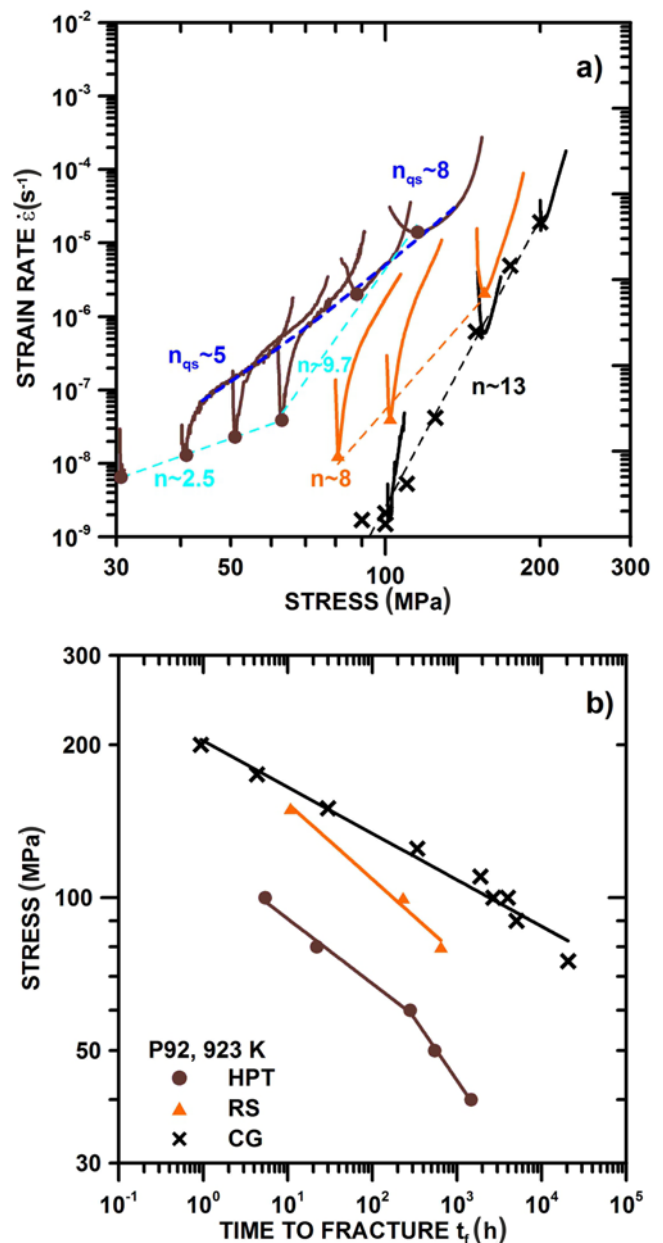


Fig. 3. Comparison of creep results for CG, RS and HPT state: a) strain rate vs. stress and b) stress vs. time to fracture.

at the high stresses. In region II, where the strain is still uniform, the softening slows down, and the values of Ω are significantly smaller than in region I. The deviation of the creep curve from the dashed line at the highest strains in region II is caused by gradual fracture processes. The influence of the local necking and fracture becomes significant only in region III.

Figure 3 shows the dependences of strain rate on the stress for CG, RS and HPT state. One can see that the stress exponent of the minimum creep rate $n = d \ln \dot{\epsilon}_{\min} / d \ln \sigma$ determined for CG state is approximately 13. The creep results (Fig. 3) demonstrate

that P92 processed by RS exhibited more or less similar $\dot{\epsilon}_{\min}$ and time to fracture (t_f) compared to CG state at the stress of 150 MPa. However, RS-processed specimens exhibited faster $\dot{\epsilon}_{\min}$ at lower stresses than CG state. The differences in $\dot{\epsilon}_{\min}$ and t_f between CG and RS states increase with the decreasing value of applied stress.

The $\dot{\epsilon}_{\min}$ for HPT-processed state is about 2 orders of magnitude faster in comparison with RS and CG states. The value of n determined for HPT-processed state decreases from $n \sim 9.7$ at stresses between 60 and 100 MPa to $n \sim 2.5$ at stresses lower than 60 MPa. The values of t_f for HPT-processed state are significantly shorter than those for CG and RS states. With respect to stress, the stress dependences are also plotted as $\dot{\epsilon}-\sigma$ creep curves from individual tensile tests at the constant load where true stress $\sigma = \sigma_0 \exp(\epsilon)$. It means that the tensile deformation is uniform, and σ (increasing with ϵ) is constant over the volume of the specimen gauge length up to the beginning of fracture processes when the stress increases mainly due to local reduction of the cross-section.

One can see that the increase of the strain rate with the stress in individual tensile tests for HPT specimens is different in comparison with stationary line related to $\dot{\epsilon}_{\min}$.

At lower stresses, where the pronounced $\dot{\epsilon}_{\min}$ was observed, the increase of $\dot{\epsilon}$ with σ in individual tensile tests is faster than the stationary line. An opposite tendency can be found at high stresses. The stress exponent determined from $\dot{\epsilon}-\sigma$ creep curves can be called the quasi-stationary stress exponent n_{qs} [7, 23]. It can be seen (Fig. 3) that the regions II shown in Fig. 2 are continuously linked together and form nearly the continuous $\dot{\epsilon}-\sigma$ dashed blue curve with n_{qs} about 5–6 at low stresses and about 8 at high stresses.

3.2. Microstructure

The microstructure of CG state after creep (Fig. 4) consists of subgrains and laths boundaries located in the interior of prior austenite grains.

Comparing microstructure (Figs. 4a,b) in the grip part and the gauge length showed that the creep strain led to the slight coarsening of microstructure in the gauge length. The local strain in the necking area situated in the proximity of the final fracture led to the formation of grains significantly elongated parallel to the direction of the applied stress (Fig. 4c).

Figures 5a,b show RS-processed microstructure in the grip part and a gauge length of the specimen tested at 923 K and 150 MPa. One can see that microstructure is significantly heterogeneous and contains fine grains placed at the boundaries of markedly elongated grains. The results also demonstrate that the microstructure at the beginning of creep testing (after annealing at 923 K for 5 h) consists of the grains with

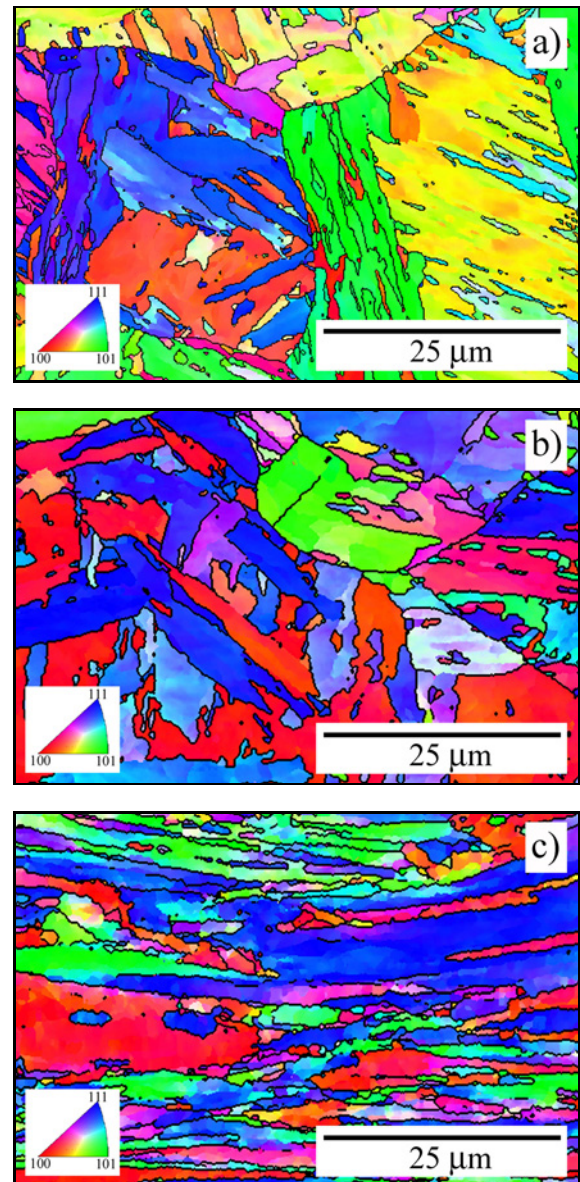


Fig. 4. Microstructure of CG P92 steel in: a) grip part, b) gauge length, and c) near the fracture.

the mean size of about 2 μm and subgrains with the mean size of about 0.75 μm . Creep testing at 150 MPa led only to the slight coarsening of microstructure (Fig. 6a).

It was observed that the microstructure coarsens significantly with increasing creep time in the grip parts and gauge lengths (Fig. 6a). The microstructure in the gauge length and area near fracture can exhibit finer size of grains and subgrains in comparison with the grip part tested for the same creep time. However, the microstructure of the RS-processed state is very inhomogeneous, and long elongated grains exceed the observed area. Therefore, the mean grain size may not be entirely accurate.

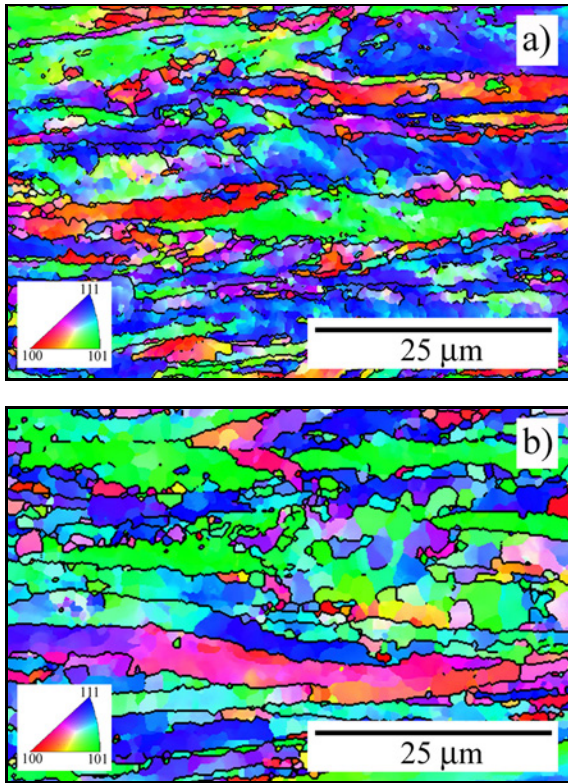


Fig. 5. Microstructure of the RS-processed state after creep at 150 MPa: a) in the grip part and b) in the gauge length.

The microstructure of the HPT-processed P92 steel contained at the beginning of the creep testing the mean grain size about 0.7 μm (Fig. 6b). The microstructure is more or less homogeneous compared to the microstructure of the RS-processed state (Fig. 7). The static annealing (microstructure in the grip parts) led only to slight coarsening (Fig. 6b). However, the creep strain caused significant coarsening of microstructure (Figs. 6b and 7). The results demonstrate (Fig. 7) that the mean grain size in the area near fracture and also in the gauge length of the HPT state tested at 923 K and 80 MPa ($t_f \sim 22$ h, $\epsilon_f \sim 0.4$) is significantly larger than the grain size in the specimen tested at 30 MPa and interrupted at $\epsilon \sim 0.05$ (creep time ~ 620 h).

4. Discussion

Many works investigate the thermal stability of UFG microstructure only after static (stress-free) annealing for relatively short times [24–27]. It seems to be sufficient because UFG are often tested for their superplastic behaviour occurring at strain rates 10^{-4} – 10^{-2} s $^{-1}$ thus, the tensile tests take only short times [28–31]. For this reason, the works investigating the high-temperature behaviour of UFG materials often

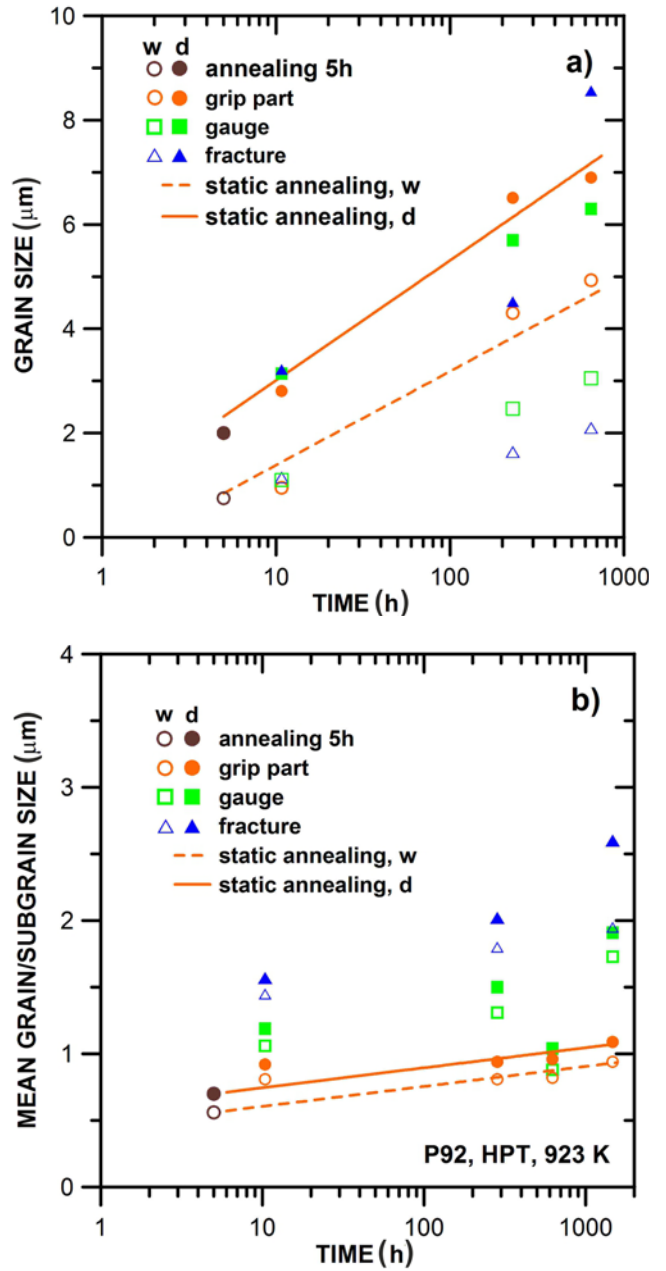


Fig. 6. Comparison of grain and subgrain size in the different locations of tensile specimens tested at 923 K, a) RS-processed and b) HPT-processed P92 steel.

consider grain size after SPD or short-term annealing [27, 30] for the determination of creep mechanisms. However, in the present work, it was observed that the microstructure coarsening during creep testing depends rather on creep strain than on creep time. It seems that the grain coarsening is limited by the stationary size of subgrains expected in coarse-grained materials (Fig. 8). The stationary subgrain size can be estimated by the following relationship:

$$w_s = k_w Gb / \sigma, \quad 10 \leq k_w \leq 30, \quad (1)$$

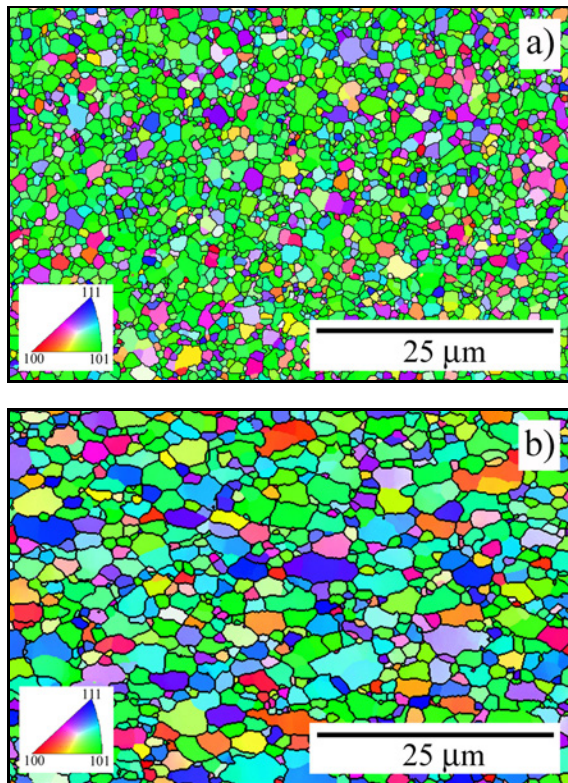


Fig. 7. Microstructure of HPT-processed state tested at a) 923 K and 30 MPa (gauge length, $\varepsilon \sim 0.05$, $t \sim 620$ h) and b) 923 K and 80 MPa (area near fracture, $\varepsilon_f \sim 0.4$, $t_f \sim 22$ h).

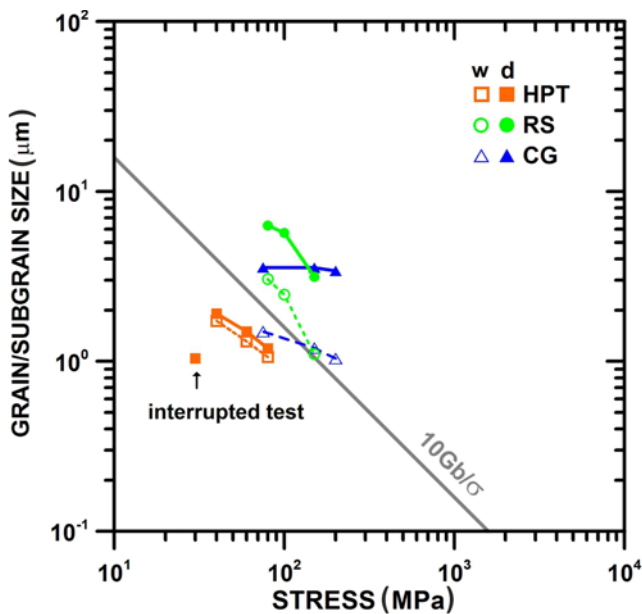


Fig. 8. Comparison of grain and subgrain size measured in the gauge lengths of CG, RS, and HPT-processed state with expected stationary subgrain size.

where $b = 2.48 \times 10^{-10}$ m [32] is the length of the Burgers vector, $G = 63.9$ GPa [33] is the shear modulus at a given temperature T , and k_w was set equal to 10.

Similar coarsening of microstructure was also observed in UFG Ti alloy during superplastic behaviour at 873 K and constant strain rate at 10^{-4} s $^{-1}$ [34] and UFG steel tested at 873 K [12]. The comparison of mean grain size for HPT-processed specimens after creep with expected stationary subgrain size w_s (Fig. 8) shows that the grains grow during creep testing up to the size near w_s .

The present results demonstrate that the grain size measured in the region near $\dot{\varepsilon}_{\min}$, for the creep test performed at 30 MPa and interrupted at strain about 0.05 (creep time about 620 h), is still near the UFG region (the region with d between 0.1–1 μm). This grain size is significantly finer than quasi-stationary subgrain size w . However, the grain size measured in gauge lengths of specimens after creep testing at higher stresses is significantly larger, although the time to fracture was significantly shorter. It means that grains coarsen mainly due to increasing creep strain. Even though the grains coarsen significantly with increasing creep strain, they do not entirely reach the expected value w_s . Moreover, the mean grain size of HPT-processed steel with decreasing applied stress becomes increasingly smaller than w_s . It seems that the ratio between the grain size during creep testing and the value of w_s is related to the value of stress exponent n and thus to the creep mechanism. In the case that the grain size during creep testing is significantly smaller in comparison with w_s ($d \sim 0.2$ – $0.4 w_s$), which was observed near $\dot{\varepsilon}_{\min}$ at low stresses, the stress exponent n is about 2–3. The value of n about 2 is usually related to the grain boundary sliding (GBS). This result suggests that the largest activity of GBS in UFG P92 may be expected at low stresses between 30–60 MPa and creep strain about 0.05. This observation seems to be consistent with the earlier study by Sklenicka et al. [35] that the largest number of boundaries begins to slip at the early stages of creep testing. However, $\dot{\varepsilon}_{\min}$ measured in low stresses seems to be much slower than that, which could be explained by GBS. Such slow $\dot{\varepsilon}_{\min}$ may be more related to diffusion creep [36].

When the grains coarsen with increasing creep strain and approach the size closer to w ($d \sim 0.5$ – $0.6 w_s$), the value of n_{qs} is about 5–8. Similar values of n_{qs} were also found in other studies investigating creep behaviour of UFG materials [6–8, 23]. This creep behaviour was explained and also experimentally modelled by using the simple dislocation model, which was proposed by Blum et al. [37]. The model is based on the storage and dynamic recovery of dislocations at high-angle grain boundaries. In the case that the grains are so fine that no subgrains are

formed in their interiors, the dislocations are recovered at HAGBs. When grain size is significantly larger than w and grains contain LAGBs in their interiors the dislocations are mainly recovered at LAGBs. In this case, the creep behaviour of SPD-processed materials approaches the creep behaviour of the CG state. This creep behaviour can be found in the RS-processed state. The stress dependence (Fig. 3a) demonstrates that $\dot{\epsilon}_{\min}$ and also t_f at 150 MPa are not significantly different in the RS-processed and CG states. The grain and subgrain sizes in the gauge lengths of the RS and CG states after creep at 150 MPa are also more or less similar (Fig. 8).

However, the RS-processed specimens tested at stresses 80 and 100 MPa exhibited significantly faster $\dot{\epsilon}_{\min}$ and shorter t_f in comparison with the CG state (Fig. 3). The microstructure of the RS-processed state at the beginning of creep testing exhibited the mean grain size slightly lower or comparable and subgrain size significantly finer than w_s (Figs. 6, 8). The microstructure results suggest that at lower stresses 80 and 100 MPa, the creep behaviour of the RS-processed state in the region about $\dot{\epsilon}_{\min}$ may be influenced by grain boundary mediated processes. This explanation can be supported by the decrease of n value which is a typical feature of the creep behaviour of UFG materials [11]. However, the heterogeneous microstructure of the RS-processed state at the beginning of creep testing also contains many LAGBs. Thus creep strength is influenced not only by HAGBs but also significantly by LAGBs, like the strength of CG state [6–8]. At creep strains higher than ~ 0.05 – 0.1 , a significant ductility improvement was observed (Fig. 2). The microstructure results suggest that ductility improvement in the RS-processed state at higher strains may be related to the microstructure coarsening.

5. Summary and conclusions

Martensitic creep-resistant P92 steel was processed by rotary swaging and high-pressure torsion at room temperature. The creep behaviour and microstructure changes in CG and SPD-processed states were investigated at 923 K and different applied tensile stresses.

The main results are as follows:

1. The CG P92 steel can exhibit at high stresses similar creep behaviour as the RS-processed state. However, the RS-processed state exhibited, at the stresses lower than 150 MPa, faster $\dot{\epsilon}_{\min}$, shorter t_f and higher ductility in comparison with CG P92 steel.

2. P92 steel processed by HPT exhibited significantly faster $\dot{\epsilon}_{\min}$ and higher ductility compared to the CG state.

3. The creep strain significantly accelerates the

coarsening of the microstructure in the HPT-processed state.

4. The grain coarsening during creep leads to the change of the stress exponent $n(n_{qs})$, thus changing the creep mechanism. The value of n depends on the ratio d/w_s . The results suggest that lower values of the ratio d/w_s lead to lower values of n .

Acknowledgements

The authors acknowledge financial support from the Czech Science Foundation (grant No. 19-18725S). The work was supported partly by a grant-in-aid from MEXT, Japan, for scientific research (A) (No. J19H00830).

References

- [1] F. Abe, T-U. Kern, R. Viswanathan, Creep-resistant steels, Woodhead Publishing, 2008. ISBN: 978-1-84569-178-3.
- [2] R. O. Kaibyshev, V. N. Skorobogatykh, I. A. Shchenkova, New martensitic steels for fossil power plant: Creep resistance, I. A. Phys. Metals Metallogr. 109 (2010) 186–200. [doi:10.1134/S0031918X10020110](https://doi.org/10.1134/S0031918X10020110)
- [3] F. Abe, Creep rates and strengthening mechanisms in tungsten-strengthened 9Cr steels, Mater. Sci. Eng. A 319–321 (2001) 770–773. [doi:10.1016/S0921-5093\(00\)02002-5](https://doi.org/10.1016/S0921-5093(00)02002-5)
- [4] N. Dudova, A. Plotnikova, D. Molodov, A. Belyakov, R. Kaibyshev, Structural changes of tempered martensitic 9%Cr-2%W-3%Co steel during creep at 650 °C, Mater. Sci. Eng. A 543 (2012) 632–639. [doi:10.1016/j.msea.2011.12.020](https://doi.org/10.1016/j.msea.2011.12.020)
- [5] K. Maruyama, K. Sawada, J. Koike, Strengthening mechanisms of creep resistant tempered martensitic steel, ISIJ International 41 (2001) 641–653. [doi:10.2355/isijinternational.41.641](https://doi.org/10.2355/isijinternational.41.641)
- [6] W. Blum, J. Dvorak, P. Kral, P. Eisenlohr, V. Sklenicka, Effect of grain refinement by ECAP on creep of pure Cu, Mater. Sci. Eng. A 590 (2014) 423–432. [doi:10.1016/j.msea.2013.10.022](https://doi.org/10.1016/j.msea.2013.10.022)
- [7] W. Blum, J. Dvorak, P. Kral, P. Eisenlohr, V. Sklenicka, Quasi-stationary strength of ECAP-processed Cu-Zr at 0.5 Tm, Metals 9 (2019) 1149. [doi:10.3390/met9111149](https://doi.org/10.3390/met9111149)
- [8] W. Blum, J. Dvořák, P. Král, P. Eisenlohr, V. Sklenička, Effects of grain refinement by ECAP on the deformation resistance of Al interpreted in terms of boundary-mediated Processes, J. Mater. Sci. Technol. 32 (2016) 1309–1320. [doi:10.1016/j.jmst.2016.08.028](https://doi.org/10.1016/j.jmst.2016.08.028)
- [9] H. Mughrabi, Revisiting “Steady-State” monotonic and cyclic deformation: emphasizing the quasi-stationary state of deformation, Metall. Mater. Trans. A 51 (2020) 1441–1456. [doi:10.1007/s11661-019-05618-x](https://doi.org/10.1007/s11661-019-05618-x)
- [10] W. Blum, P. Eisenlohr, Structure evolution and deformation resistance in production and application of nanostructured materials. The concept of steady-state grains, Mater. Sci. Forum 683 (2011) 163–181. [doi:10.4028/www.scientific.net/MSF.683.163](https://doi.org/10.4028/www.scientific.net/MSF.683.163)
- [11] P. Kral, J. Dvorak, V. Sklenicka, T. G. Langdon, The characteristics of creep in metallic materials processed

- by severe plastic deformation, *Mater. Trans.* 60 (2019) 1506–1517. [doi:10.2320/matertrans.MF201924](https://doi.org/10.2320/matertrans.MF201924)
- [12] P. Král, J. Dvořák, W. Blum, V. Sklenička, Z. Horita, Y. Takizawa, Y. Tang, L. Kunčická, R. Kocich, M. Kvapilová and M. Svobodová, The effect of predeformation on creep strength of 9% Cr steel, *Materials* 13 (2020) 5330. [doi:10.3390/ma13235330](https://doi.org/10.3390/ma13235330)
- [13] V. Sklenička, K. Kuchařová, M. Svobodová, M. Kvapilová, P. Král, L. Horváth, Creep properties in similar weld joint of a thick-walled P92 steel pipe, *Mater. Character.* 119 (2016) 1–12. [doi:10.1016/j.matchar.2016.06.033](https://doi.org/10.1016/j.matchar.2016.06.033)
- [14] K. Nam, Y. He, K. Shin, Microstructural evolution of super304H upon ultrasonic shot peening and subsequent annealing, *J. Nanosci. Nanotechnol.* 18 (2018) 6274–6277. [doi:10.1166/jnn.2018.15632](https://doi.org/10.1166/jnn.2018.15632)
- [15] R. Z. Valiev, R. K. Islamgaliev, I. V. Alexandrov, Bulk nanostructured materials from severe plastic materials, *Prog. Mater. Sci.* 45 (2000) 103–189. [doi:10.1016/S0079-6425\(99\)00007-9](https://doi.org/10.1016/S0079-6425(99)00007-9)
- [16] N. Tsuji, R. Gholizadeh, R. Ueji, N. Kamikawa, L. Zhao, Y. Tian, Y. Bai, A. Shibata, Formation mechanism of ultrafine grained microstructures: Various possibilities for fabricating bulk nanostructured metals and alloys, *Mater. Trans.* 60 (2019) 1518–1532. [doi:10.2320/matertrans.MF201936](https://doi.org/10.2320/matertrans.MF201936)
- [17] V. Sklenička, K. Kuchařová, P. Král, K. Kvapilová, M. Svobodová, J. Čmakal, The effect of hot bending and thermal ageing on creep and microstructure evolution in thick-walled P92 steel pipe. *Mater. Sci. Eng. A* 644 (2015) 297–309. [doi:10.1016/j.msea.2015.07.072](https://doi.org/10.1016/j.msea.2015.07.072)
- [18] L. Kunčická, R. Kocich, J. Dvořák, A. Macháčková, Rotary swaged laminated Cu-Al composites: Effect of structure on residual stress and mechanical and electric properties, *Mater. Sci. Eng.* 742 (2019) 743–750. [doi:10.1016/j.msea.2018.11.026](https://doi.org/10.1016/j.msea.2018.11.026)
- [19] A. Macháčková, L. Krátká, R. Petrmičl, L. Kunčická, R. Kocich, Affecting structure characteristics of rotary swaged tungsten heavy alloy via variable deformation temperature. *Materials* 12 (2019) 4200. [doi:10.3390/ma12244200](https://doi.org/10.3390/ma12244200)
- [20] P. Kral, J. Dvorak, V. Sklenicka, T. Masuda, Z. Horita, K. Kucharova, M. Kvapilova, M. Svobodova, Microstructure and creep behaviour of P92 steel after HPT, *Mater. Sci. Eng.* 723 (2018) 287–295. [doi:10.1016/j.msea.2018.03.059](https://doi.org/10.1016/j.msea.2018.03.059)
- [21] V. Sklenicka, P. Kral, J. Dvorak, Y. Takizawa, T. Masuda, Z. Horita, K. Kucharova, M. Kvapilova, M. Svobodova, Effects of grain refinement and predeformation impact by severe plastic deformation on creep in P92 martensitic steel, *Adv. Eng. Mater.* 22 (2019) 1900448. [doi:10.1002/adem.201900448](https://doi.org/10.1002/adem.201900448)
- [22] F. Abe, Effect of fine precipitation and subsequent coarsening of Fe₂W Laves phase on the creep deformation behavior of tempered martensitic 9Cr-W steels, *Metall. Mater. Trans.* 36A (2005) 321–332. [doi:10.1007/s11661-005-0305-y](https://doi.org/10.1007/s11661-005-0305-y)
- [23] W. Blum, J. Dvořák, P. Král, P. Eisenlohr, V. Sklenička, Strain rate contribution due to dynamic recovery of ultrafine-grained Cu-Zr as evidenced by load reductions during quasi-stationary deformation at 0.5T_m, *Metals* 9 (2019) 1150. [doi:10.3390/met9111150](https://doi.org/10.3390/met9111150)
- [24] H. Hasegawa, S. Komura, A. Utsunomiya, Z. Horita, M. Furukawa, M. Nemoto, T. G. Langdon, Thermal stability of ultrafine-grained aluminum in the presence of Mg and Zr additions, *Mater. Sci. Eng. A* 265 (1999) 188–196. [doi:10.1016/S0921-5093\(98\)01136-8](https://doi.org/10.1016/S0921-5093(98)01136-8)
- [25] W. Q. Cao, A. Godfrey, W. Liu, Q. Liu, EBSD study of the annealing behavior of aluminum deformed by equal channel angular processing, *Mater. Sci. Eng. A* 360 (2003) 420–425. [doi:10.1016/S0921-5093\(03\)00508-2](https://doi.org/10.1016/S0921-5093(03)00508-2)
- [26] P. H. R. Pereira, Y. Huang, T. G. Langdon, Examining the thermal stability of an Al-Mg-Sc alloy processed by high-pressure torsion, *Mater. Research* 20 (2017) 39–45. [doi:10.1590/1980-5373-mr-2017-0207](https://doi.org/10.1590/1980-5373-mr-2017-0207)
- [27] P. B. Berbon, S. Komura, A. Utsunomiya, Z. Horita, M. Furukawa, M. Nemoto, T. G. Langdon, An evaluation of superplasticity in aluminum-scandium alloys processed by equal-channel angular pressing, *Mater. Trans. JIM* 40 (1999) 772–778. [doi:10.2320/matertrans1989.40.772](https://doi.org/10.2320/matertrans1989.40.772)
- [28] A. Alhamidi, Z. Horita, Grain refinement and high strain rate superplasticity in aluminium 2024 alloy processed by high-pressure torsion, *Mater. Sci. Eng. A* 622 (2015) 139–145. [doi:10.1016/j.msea.2014.11.009](https://doi.org/10.1016/j.msea.2014.11.009)
- [29] H. Matsunoshita, K. Edalati, M. Furui, Z. Horita, Ultrafine-grained magnesium-lithium alloy processed by high-pressure torsion: Low-temperature superplasticity and potential for hydroforming, *Mater. Sci. Eng. A* 640 (2015) 443–448. [doi:10.1016/j.msea.2015.05.103](https://doi.org/10.1016/j.msea.2015.05.103)
- [30] T. J. Lee, Y. B. Park, W. J. Kim, Importance of diffusional creep in fine grained Mg-3Al-1Zn alloys, *Mater. Sci. Eng. A* 580 (2013) 133–141. [doi:10.1016/j.msea.2013.04.061](https://doi.org/10.1016/j.msea.2013.04.061)
- [31] M. Kawasaki, T. G. Langdon, Review: Achieving superplastic properties in ultrafine-grained materials at high temperatures, *J. Mater. Sci.* 51 (2016) 19–32. [doi:10.1007/s10853-015-9176-9](https://doi.org/10.1007/s10853-015-9176-9)
- [32] H. J. Frost, M. F. Ashby, *Deformation-Mechanism Maps*. Pergamon Press, Oxford, UK, 1982. pp. 62–63. ISBN: 978-0080293387
- [33] K. Sawada, M. Takeda, K. Maruyama, R. Ishii, M. Yamada, Y. Nagae, R. Komine, Effect of W on recovery of lath structure during creep of high chromium martensitic steels, *Mater. Sci. Eng. A* 267 (1999) 19–25. [doi:10.1016/S0921-5093\(99\)00066-0](https://doi.org/10.1016/S0921-5093(99)00066-0)
- [34] P. Kral, J. Dvorak, W. Blum, E. Kudryavtsev, S. Zherebtsov, G. Salishchev, M. Kvapilova, V. Sklenicka, Creep study of mechanisms involved in low-temperature superplasticity of UFG Ti-6Al-4V processed by SPD, *Mater. Character.* 116 (2016) 84–90. [doi:10.1016/j.matchar.2016.04.007](https://doi.org/10.1016/j.matchar.2016.04.007)
- [35] V. Sklenička, High temperature intergranular damage and fracture, *Mater. Sci. Eng. A* 234 (1997) 30–36. [doi:10.1016/S0921-5093\(97\)00172-X](https://doi.org/10.1016/S0921-5093(97)00172-X)
- [36] P. Kral, J. Dvorak, V. Sklenicka, T. Masuda, Z. Horita, K. Kucharova, M. Kvapilova, M. Svobodova, The effect of ultrafine-grained microstructure on creep behaviour of 9% Cr steel, *Materials* 11 (2018) 787. [doi:10.3390/ma11050787](https://doi.org/10.3390/ma11050787)
- [37] W. Blum, X. H. Zeng, A simple dislocation model of deformation resistance of ultrafine-grained materials explaining Hall-Petch strengthening and enhanced strain rate sensitivity, *Acta Mater.* 57 (2009) 1966–1974. [doi:10.1016/j.actamat.2008.12.041](https://doi.org/10.1016/j.actamat.2008.12.041)